INSTITUTE OF PHYSICS PUBLISHING PLASMA PHYSICS AND CONTROLLED FUSION

Plasma Phys. Control. Fusion **44** (2002) 351–359 PII: S0741-3335(02)30471-8

Coherent structures in the edge turbulence of the CASTOR tokamak

E Martines[1], **M Hron**[2] **and J Stöckel**[2]

[1] Consorzio RFX, Associazione Euratom-ENEA sulla Fusione, Padova, Italy
[2] Institute of Plasma Physics, Czech. Acad. Sci., Association EURATOM/IPP.CR, Prague, Czech Republic

E-mail: martines@igi.pd.cnr.it

Received 5 November 2001, in final form 23 January 2002
Published 4 March 2002
Online at stacks.iop.org/PPCF/44/351

Abstract

A two-dimensional array of electric probes placed on the poloidal plane has been inserted in the edge region of the CASTOR tokamak. The floating potential patterns measured by the probes show the presence of localized structures which are convected poloidally by the $\boldsymbol{E} \times \boldsymbol{B}$ plasma motion. The lifetime of these structures has been found to be large enough to allow them to complete several full poloidal rotations before dying away. Furthermore, the eddy turnover time of the plasma around the potential blobs is smaller than the lifetime, so that these structures can be called coherent.

1. Introduction

The confinement properties of tokamaks and other toroidal devices for the formation of fusion-relevant plasmas are well known to be determined by turbulence-induced transport processes [1]. The understanding of the turbulence dynamics in this kind of plasmas is, therefore, of primary importance to attain the ultimate goal of a first-principles modelling of these processes. In recent years, particular attention has been paid to the shape of the structures which may be identified in the turbulence. This attention has emerged from the observation that turbulence-driven radial transport is bursty, i.e. the flux is characterized by a probability distribution function (PDF) which exhibits very long tails [2]. These tails, which correspond to strong transport events, can be associated to particular types of turbulent structures. In particular, several authors have suggested that they could be identified with the avalanches of self-organized critical (SOC) systems, although some other groups have recently questioned the applicability of the SOC paradigm to the edge of fusion devices [3–5].

The crucial role played by coherent structures in determining the turbulence dynamics is well known in neutral fluid turbulence [6, 7]. In particular, the influence of coherent structures on transport processes has been identified as a very relevant one [8]. This fact suggests that for

a better understanding of transport in fusion plasmas, a clear understanding of the role played by coherent structures in the turbulence present in such devices might be crucial.

Several authors in the past have looked experimentally for the presence of coherent structures in the edge region of fusion devices. An important work in this field was that of Zweben [9], who used a two-dimensional array of probes similar to the one described in the present paper to study the spatial structure of density fluctuations in the edge of the Caltech tokamak. He identified density 'blobs' which travelled both poloidally and radially, with an estimated average lifetime equal to about 1–2 times the autocorrelation time of single-probe data, although a minority of the blobs had longer lifetimes. In the end, this work was inconclusive about the presence of coherent structures, and called for more detailed measurements and analyses.

More recently, Benkadda *et al* [10] used the biorthogonal decomposition applied to the signals of poloidal arrays of probes to infer the presence of large-scale coherent structures in the ASDEX and ADITYA tokamaks. The structures, propagating poloidally in the ion diamagnetic drift direction, were found to play a dominant role in determining the transport in the scrape off layer and to give rise to the non-Gaussianity of the PDF of the signals.

In the ADITYA tokamak, further observations of coherent structures have been put forward by Joseph *et al* [11] using the conditional averaging technique. The structures, detected with a poloidal array of probes, have a typical size of 2 cm radially and 5 cm poloidally.

A careful analysis of measurements made with a poloidal array of probes in the edge region of ASDEX by Endler *et al* [12] led to a picture of eddies elongated along the magnetic field and poloidally and radially localized within a few centimetres. The estimated lifetime of these eddies allowed however for only half a turn before their decay. The phase difference between potential and density fluctuations suggested that the eddies were transporting mass across the magnetic field from high-density to low-density regions.

Dong *et al* [13] have used correlation analysis and the study of the PDFs of H_α emission measurements to infer the presence of coherent structures in the edge of the CT-6B tokamak. These structures, which did not show any radial propagation, were found to have a radial extension of 1 cm or more and a lifetime of 20–100 μs.

The experimental evidence cited above is also supported by theoretical and numerical work, which shows the possibility of the formation of coherent structures in drift wave turbulence [14–16].

In this paper, we report the detection, made using a two-dimensional array of probes, of coherent structures in the edge region of the CASTOR tokamak. The paper is organized as follows: in section 2, the experimental setup is presented; in section 3, the various data analysis techniques are described and the experimental results are presented; in section 4, a discussion of the experimental results is given, with particular emphasis on the notion of coherent structure; finally, in section 5, the conclusions are drawn.

2. Experimental setup

The experimental results described in this paper have been collected in the CASTOR tokamak, operating in Prague. CASTOR is a small-sized tokamak, with a major radius of 400 mm and a minor radius of 100 mm. The plasma column radius is determined by a poloidal ring limiter with a radius of 85 mm. The plasma column radius is actually smaller (around 65 mm) because the plasma is shifted downwards. The toroidal magnetic field in the discharges described here was 1 T, and the plasma current was 9 kA. The typical discharge duration was 35 ms.

The data have been collected using a two-dimensional array of 64 electric probes, arranged in a regular pattern of 8×8. The experimental setup is depicted schematically in figure 1. Each probe is a graphite pin with a radius of 2 mm, flush-mounted in a boron nitride front plate.

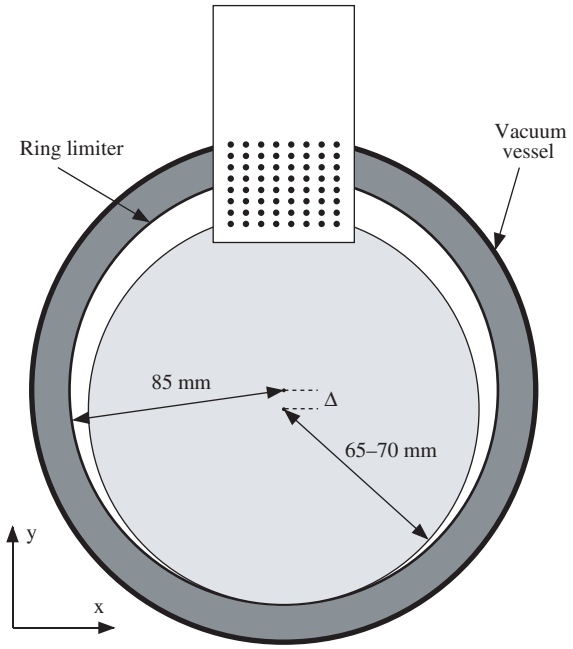

Figure 1. Scheme of the experimental setup. The picture shows a scheme of the poloidal section of the CASTOR tokamak where the array of probes has been inserted. The plasma, shifted downwards, is also depicted.

The front plate is inserted in a supporting structure made of stainless steel, covered by a boron carbide coating applied by plasma spraying. The structure is inserted in the plasma in the top side of the torus, with the front plate and the pins located on the poloidal plane (i.e. the toroidal field is normal to the plate). It is possible to consider the array as made of 8 columns of 8 pins each, vertically aligned. If the curvature of the machine is neglected, the rows of pins can be considered to be aligned with the poloidal direction and the columns with the radial direction. The Cartesian coordinate system shown in figure 1 is used in the paper, with the origin placed in the centre of the vacuum vessel section. The distance between adjacent pins is 6 mm horizontally and 4.5 mm vertically, so that the array covers a rectangular region of 42×22.5 mm. The overall size of the system is 56×94 mm in the poloidal plane. This area occupied by this object is not negligible if compared to the total poloidal section, and the effect on the plasma will be discussed below. The thickness of the system (in the toroidal direction) is 18 mm.

In the campaign described in this paper, only the six most inserted rows of pins were used, for a total of 48 probes. All the probes were left electrically floating, and the floating potential V_f was sampled at a frequency of 1 MHz. A moving average with a window of 201 samples is subtracted from the signals prior to the analysis. This treatment corresponds to a high-pass filtering which isolates the fluctuations discarding the slow equilibrium evolution.

3. Detection of long-living structures

The first analysis of the data collected by the two-dimensional array has been performed simply by building 'movies' from the measurements [17]. These movies display localized structures ('blobs') of floating potential which propagate in the poloidal direction. The propagation

direction is the ion diamagnetic drift direction, and also the direction of the $\boldsymbol{E} \times \boldsymbol{B}$ motion due to the radial electric field. Indeed, the radial electric field is positive in the SOL and negative inside the last closed flux surface (LCFS), which is located at $r = 65$–70 mm.

The typical floating potential patterns seen by the probes can be visualized by considering only one column of probes. Such a subset of probes is equivalent to using a radial array ('rake probe'). In particular, the eighth column of probes will be considered. This is the most upstream one with respect to the $\boldsymbol{E} \times \boldsymbol{B}$ plasma rotation, and therefore the one less subject to perturbation effects caused by the array supporting structure.

A typical time evolution of the signals collected by the probe column is shown in figure 2. The data are depicted using a colour coding, with blue indicating negative values and red indicating positive values. The peak values are ± 27 V. The figure shows the presence of structures which extend in the radial direction for about 1 cm. Furthermore, it is possible to identify a quasi-periodicity in the way in which the structures appear on the probe column under study. For example, in the case under study, a group of several negative structures clustered together appears several times. Also the positive structures seem to appear at regular intervals.

A confirmation of the presence of periodicity is given by the autocorrelation function. In order to enhance the effect of the radially extended structures, the autocorrelation function has been computed on the average of the signals of the three most inserted probes of the eighth column. The result is shown in figure 3. An oscillating behaviour is clearly seen on the function, well above the significance level, which is shown by two horizontal dotted lines. The oscillation is convolved with a decay, which has been found to have the shape of a power law. Indeed, the dashed curve in figure 3 is the result of a fit with a function of the kind $f(\tau) = (\tau/\tau_0)^{\alpha} \cos(\omega\tau)$. The curve fits the data well with an oscillation frequency $\omega/2\pi = 7.7$ kHz and a decay exponent $\alpha = -0.32$. It is worth noting that an exponentially decaying curve, which has also been attempted, does not give such a good fit. The power-law decay is in agreement with previous findings of long-range correlations in the turbulence measurements in the edge of fusion devices [18]. Other fits, performed on different estimates of the autocorrelation function obtained in other discharges and time intervals, have given values of α ranging between -0.3 and -0.5. The rotation frequency obtained from the fit in figure 3 corresponds to a poloidal velocity of $3.4\ \mathrm{km\ s^{-1}}$, compatible with the $\boldsymbol{E} \times \boldsymbol{B}$ velocity. This confirms the hypothesis that some turbulent structures are convected poloidally, living long enough to execute several poloidal revolutions.

Based upon the elements presented up to now, the analysis has been continued under the assumption of frozen structures convected poloidally by the $\boldsymbol{E} \times \boldsymbol{B}$ plasma motion. Such an assumption allows to map the time evolution shown in figure 2 to the poloidal plane, assuming a rigid rotation of the plasma at constant angular velocity. Figure 4 shows two

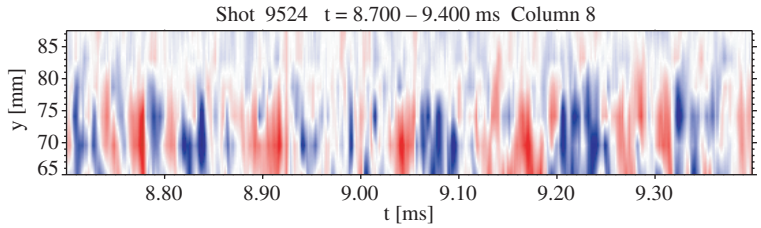

Figure 2. Floating potential measured by one column of probes plotted as a function of time and radial position. Blue indicates negative values and red indicates positive values. The peak values are ± 27 V.

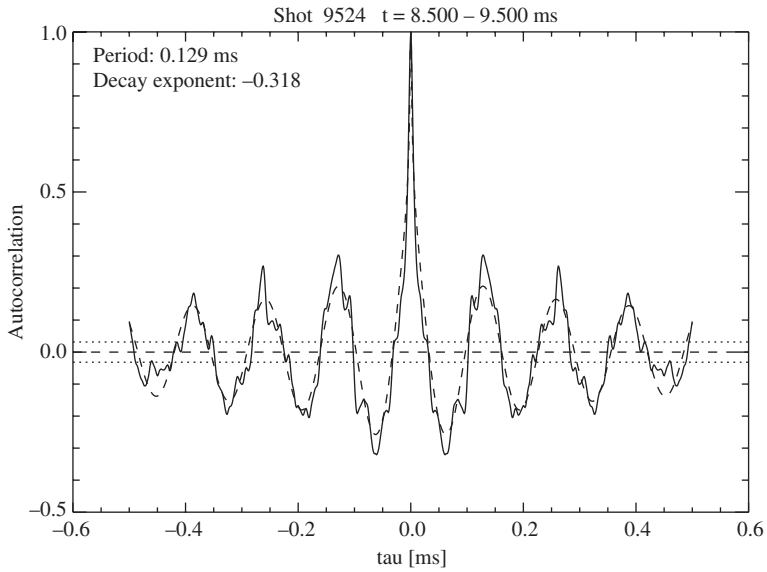

Figure 3. Autocorrelation function of the average of the three most inserted probes from the most upstream column. The dotted horizontal lines give the noise threshold. The dashed line is a fit with a function of the type $f(\tau) = (\tau/\tau_0)^{\alpha} \cos(\omega\tau)$.

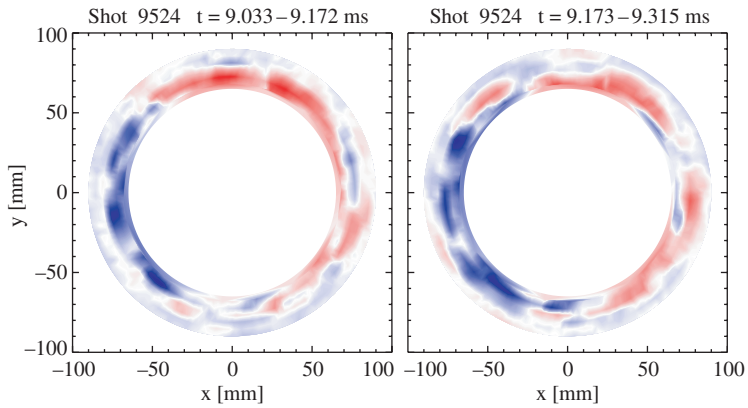

Figure 4. Floating potential measured by one column of probes mapped to the poloidal plane assuming a constant plasma rotation velocity and frozen turbulence. The two pictures refer to two subsequent rotation periods. The estimated position of the LCFS is $r = 65$–70 mm.

examples of such a mapping. The two images correspond to two different and subsequent time intervals, each lasting about 140 μs, i.e. the duration corresponding to one poloidal turn. The most interesting feature observed in this figure is that the two images have many features in common, such as the three blue (negative) structures on the left. This further confirms that the underlying assumption of frozen turbulence is verified, and that large-scale structures living several hundreds of microseconds exist in the CASTOR edge.

In order to obtain a visualization of the typical behaviour of the potential structures, the conditional averaging technique has been used. One of the probes of the array, namely the one in row 4 and column 4, has been taken as a reference to detect the events corresponding to

the passage of structures. One event is detected every time the reference signal goes above a fraction β of its standard deviation. Alternatively, for negative structures, one event is detected every time the signal goes below $-\beta$ times its standard deviation. Typically, the value $\beta = 1.5$ has been used. The results are anyway not at all sensitive to the actual value of β. When the event is detected, the 8×6 array of the measurements of all the probes at that time (which we call frame) is stored. The same is done for the frames having some positive and negative time lags with respect to the event. At the end of the procedure, all the stored frames are averaged (for each value of the time lag). This yields, for zero lag, the average shape of the structures giving rise to the event. The averages at non-zero time lags yield the time evolution of this average structure.

A typical result of the conditional averaging technique is shown in figure 5. Here negative structures have been identified. The process has been carried out over an 8 ms interval in discharge 9520. 107 events have been used to build the average. The figure clearly shows that the average structure has a radial extension of 1 cm, and a poloidal extension of 3 cm, i.e. it is poloidally elongated. Its motion in the $\boldsymbol{E} \times \boldsymbol{B}$ direction, corresponding to a motion from the right to the left in the figure, is clearly seen. The motion velocity is 3–4 km s^{-1}, consistent with the estimates given above. The structures tend to be somehow less defined in the frames that are more temporally distant from the one at zero time lag: this is to be expected, due to the decay in coherence with time.

The magnitude of the average structure shown in figure 5 is 7 V. The typical root mean square (RMS) value of the floating potential signals, after subtracting the slow trend, is 10 V (or less, depending on the radial position). Thus, the uncertainty on the average, computed as

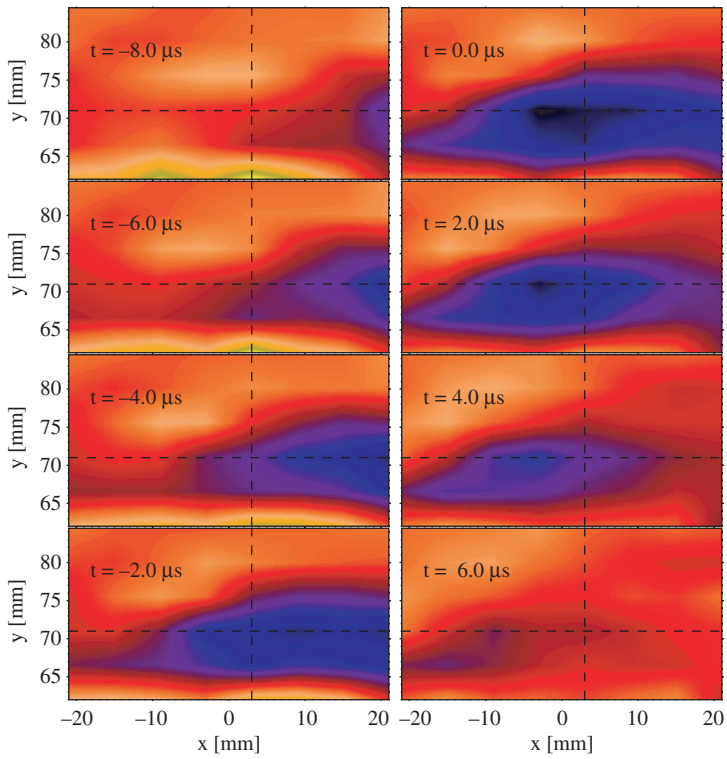

Figure 5. Conditionally averaged data showing the average negative structure at different times, relative to the detection time. The estimated position of the LCFS is $r = 65$–70 mm.

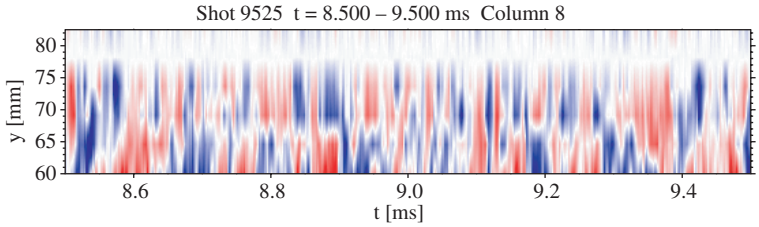

Figure 6. Floating potential measured by one column of probes plotted as a function of time and radial position (as in figure 2). Blue indicates negative values and red indicates positive values. The peak values are ± 31.4 V. The presence of the LCFS at $y \approx 68$ cm is seen as a white line separating structures of opposite polarity.

this RMS value divided by the square root of the number of events, is equal or smaller than 1 V. This result shows that the conditionally averaged structure is indeed a statistically significant feature.

Let us now turn to the issue of the perturbing effect of the array in the plasma and its turbulence. The data presented above have been obtained with the array immersed in the scrape off layer created by the downward shift of the plasma. The array is large enough to be able to act as a limiter. It was therefore expected that a deeper insertion would shift the plasma downwards, and that the turbulence seen by the array would always have the same features. This is not at all the case. It is found that the array is indeed able to penetrate the separatrix, and to diagnose the confined plasma. This is evidenced by a clear change in the turbulence characteristics. An example of this behaviour is seen in figure 6, which was obtained in the same fashion as figure 2, i.e. from the signals of the most upstream column, but with the array pushed 5 mm further inside the plasma. The presence of a separation between two regions, located at $y \approx 68$ mm, is clearly seen. As a general rule, it is found that the turbulent structures have a dipole character, with a potential peak at $y > 68$ mm corresponding to a well at $y < 68$ mm, and vice versa. The origin of this dipole-like behaviour is not clear, but is seems reasonable to conclude that it is induced by the LCFS, and that the array is indeed able to diagnose the plasma both outside and inside this surface. It is interesting to observe that, although the dipole character is the general rule, sometimes more elongated structures, able to penetrate the LCFS, are seen. It is worth noting that the same kind of dipole structures can be seen on data obtained with a rake probe, which is much less perturbative than the two-dimensional array.

4. Discussion

The data presented in the previous sections clearly show that the electrostatic turbulence in the edge of CASTOR is dominated by large-scale structures with a lifetime long enough to be able to make several poloidal revolutions. Nevertheless, this result is not enough by itself to qualify them as coherent structures. The definition of a coherent structure is somehow ambiguous. In the following, we shall define a coherent structure as a vortex-like plasma region which lives long enough to allow the plasma to complete at least one full rotation around its centre. In other words, it is a structure with a lifetime larger than its 'eddy turnover time'. This definition is borrowed from neutral fluid turbulence, and it appears to be well suited in a context, as the present one, where the measured quantity is the potential. Indeed, a blob of potential gives rise to a pattern of electric field departing from its centre (or converging to it). This in turn gives rise to an eddy-like motion in the plane perpendicular to the magnetic field due to the $\boldsymbol{E} \times \boldsymbol{B}$

motion. The definition used is also important in relation to fusion studies, since an eddy-like motion gives rise to a convective cell which can be responsible for cross-field transport of mass or energy.

The lifetime of the structures identified above has been found to be several hundreds of microseconds. This should be compared to the eddy turnover time τ. Calling δ the typical size of the structures, and v the typical velocity of the eddy motion, the eddy turnover time is given by $\tau \sim \delta/v$. The electric field associated to a structure with peak potential ϕ, is $E \sim \phi/\delta$, and the resulting eddy velocity is $v \sim E/B \sim \phi/B\delta$. Thus, the eddy turnover time can be estimated as $\tau \sim B\delta^2/\phi$. In the present case, $\phi \approx 30\,\mathrm{V}$ and $\delta < 5\,\mathrm{cm}$. This latter value is an upper limit for the poloidal direction, which is the one along which the structures extend most. Finally, τ is smaller (probably in a substantial way) than $80\,\mu\mathrm{s}$. This is smaller than the structure's lifetime. The conclusion is that the potential structures measured in the edge of CASTOR are indeed coherent structures. It is interesting to remark that this result is different from that obtained in the ASDEX tokamak, where the typical estimated lifetime of the structures was only half of the eddy turnover time [12]. It will be important, by comparing measurements performed on different devices, to find out if this discrepancy is only due to the method adopted to estimate the lifetime, or if it indicates a progressive trend towards a loss of coherence in the turbulence of larger and hotter machines.

The size of the structures observed in CASTOR, of 1 cm in the radial direction and a few cm in the poloidal one, is in line with results reported in other experiments [11–13]. It is important to remark that no clear radial propagation of the structures was observed. This goes along with the observations made in the CT-6B tokamak [13], but is in contrast with what was found in the Caltech tokamak [9], where radially moving structures were observed, although no preference for an outward average motion was detected.

An important point which requires clarification is whether the structures described in this paper are truly electrostatic in nature, or if they are associated to MHD phenomena. Unfortunately, no Mirnov coil measurements were avalaible during the two-dimensional array campaign. However, past measurements show that the typical MHD phenomena observed on CASTOR are dominated by an $m = 2$ mode at frequencies around 50–100 kHz [19]. This frequency range is substantially higher than that of the coherent structures described here, and also the poloidal wavelength is higher. It is not possible to completely exclude that other modes with the correct frequency and spatial periodicity, related to the coherent edge activity, are present in the broadband residual magnetic spectrum. This issue will be the subject of further future investigations.

5. Conclusions

The study presented in this paper clearly shows that in the edge of a small tokamak like CASTOR, the electrostatic turbulence is not fully incoherent, but is rather dominated by large-scale coherent structures. This result, which goes well along with previous findings in other tokamaks, suggests that the tokamak edge region is not in a completely disordered state. This may be due to instabilities which do not reach a fully non-linear state, or to the presence of an inverse energy cascade towards the large scales, as deduced from three-wave coupling analysis of probe data in the TEXT tokamak [20]. In any case, several experiments have reported a consistent transport associated with these structures [10, 12]. This suggests that by targeting and destroying these structures by suitable means, it should be possible to achieve consistent transport reductions. Such an approach would be less energetically demanding of the usual method of tearing apart turbulent structures through the creation of a velocity shear in the plasma.

Acknowledgments

We warmly thank Frantisek Jiranek (chief designer and construction of mechanical parts), Karel Rieger and Josef Zelenka (wires and circuits) of CASTOR for their excellent technical assistance.

References

[1] Carreras B A 1997 *IEEE Trans. Plasma Sci.* **25** 1281
[2] Carreras B A *et al* 1996 *Phys. Plasmas* **3** 2664
[3] Krommes J A and Ottaviani M 1999 *Phys. Plasmas* **6** 3731
[4] Spada E *et al* 2001 *Phys. Rev. Lett.* **86** 3032
[5] Antoni V *et al* 2001 *Phys. Rev. Lett.* **87** 045001
[6] Hussain A K M F 1983 *Phys. Fluids* **26** 2816
[7] Van Atta C W 1994 *Turbulence. A Tentative Dictionary (NATO ASI Series B: Physics vol 341)* ed P Tabeling and O Cardoso (New York: Pergamon Press) p 97
[8] Robinson S K 1991 *Ann. Rev. Fluid Mech.* **23** 601
[9] Zweben S J 1985 *Phys. Fluids* **28** 974
[10] Benkadda S, Dudok de Wit T, Vergal A, Sen A, ASDEX team and Garbet X 1994 *Phys. Rev. Lett.* **73** 3403
[11] Joseph B K, Jha R, Kaw P K, Mattoo S K, Rao V S, Saxena Y C and the Aditya team 1997 *Phys. Plasmas* **4** 4292
[12] Endler M, Niedermeyer H, Giannone L, Holzhaner E, Rudyj A, Theimer G, Tsois N and ASDEX team 1995 *Nucl. Fusion* **35** 1307
[13] Dong L, Wang L, Feng C, Li Z, Zhao Q and Wang G 1998 *Phys. Rev.* E **57** 5929
[14] Ferro Fontán C and Verga A 1995 *Phys. Rev.* E **52** 6717
[15] Naulin V and Spatschek K H 1997 *Phys. Rev.* E **55** 5883
[16] Kuvshinov B N, Pegoraro F, Rem J and Schep T J 1999 *Phys. Plasmas* **6** 713
[17] Examples of these movies can be obtained from the web site http://pc133.ipp.cas.cz/∼hron/turb/html
[18] Carreras B A *et al* 1998 Phys. Plasmas **5** 3632
Carreras B A *et al* 1999 *Phys. Plasmas* **6** 1885
[19] Stöckel J *et al* 1999 *Plasma Phys. Control. Fusion* **41** A577
[20] Ritz Ch P, Powers E J and Bengtson R D 1989 *Phys. Fluids* B **1** 153